However, despite several efforts[5], no effective inhibitors of MBLs are available.

Most members of our current antibiotic arsenal originate from screens of naturally occurring chemicals produced by soil microorganisms[6]. King and colleagues reasoned that replication of this approach might lead to the discovery of small molecules that could resensitize bacteria to drugs against which they have developed resistance. The authors performed a screen of naturally occurring microbial extracts to find compounds that could inhibit an MBL called New Delhi metallo-β-lactamase 1 (NDM-1).

Their screen identified one compound, aspergillomarasmine A (found in an extract from the fungus *Aspergillus versicolor*), that could restore the efficiency of meropenem, a carbapenem, against *E. coli* strains producing NDM-1. Aspergillomarasmine A has previously been shown to inhibit angiotensin-converting enzyme (ACE), which is produced in the body and causes blood-vessel constriction, increasing blood pressure. ACE is a zinc-dependent metalloproteinase and shares some functional similarities with MBLs, which suggests that aspergillomarasmine A might inhibit NDM-1 by interacting with zinc ions. Indeed, the authors found that aspergillomarasmine A removes zinc ions from NDM-1 in the same fashion as other known metal-binding molecules that interact with MBLs[7] (Fig. 1b).

King and colleagues tested the ability of their compound to combat resistance in 229 MBL-expressing strains of bacteria that had been isolated from patients over 10 years, from various parts of the globe. When used in combination with meropenem, they found that aspergillomarasmine A restored antibiotic susceptibility in 88% of NDM-1-producing strains of enterobacteria. Remarkably, in mice infected with a lethal strain of *K. pneumoniae* that produces NDM-1, a single-dose treatment of aspergillomarasmine A and meropenem led to a survival rate of more than 95% after 5 days of infection.

The authors showed that aspergillomarasmine A is selective — it has potent activity against NDM-1 and another MBL, Verona integron-encoded metallo-β-lactamase 2 (VIM-2), but much weaker activity against ACE. Unfortunately, aspergillomarasmine A is also ineffective against other anti-carbapenem enzymes, which, if this treatment were rolled out, might become more common, leading to resistance again. Furthermore, treatments involving compounds that aim to remove zinc ions from MBLs might inhibit the body's own metalloenzymes, causing serious side effects. However, a previous study[8] demonstrated that mice treated with aspergillomarasmine A had few side effects, and on average showed no change in arterial blood pressure. Although this is encouraging, the effects on other mammalian enzymes should be tested before drugs based on this premise are developed.

King and co-workers' study re-emphasizes the fact that drug–inhibitor combinations can be used to address the problem of increasing antibiotic resistance, through extending the lifespan of existing antibiotics. Theoretically, this approach could be applied to any resistance mechanism that affects the treatment of disease. However, many pathogens harbour more than one mechanism that confers resistance to a given drug class[9]. For example, efflux pumps in the cell membrane remove toxic chemicals (including most classes of antibiotic) from the cell, and a single inhibitor cannot address this problem as well as other resistance mechanisms, such as modification of the antibiotic's target or enzymatic degradation of the drug. Such multi-pronged resistance means that the future of antimicrobial chemotherapy will have to rely on combinations of drugs with different targets, as is the case for therapies for cancer and viral infections.

Designing new antibacterial drugs is not an easy task, requiring the development of synthetic chemicals combined with exploration of naturally occurring compounds. But the reservoir of natural products with the potential to act as antibacterial drugs has not yet been exhausted. In contrast to general thinking by drug companies, screening for such products may well still have a bright future. ■

Djalal Meziane-Cherif *and* **Patrice Courvalin** *are in the Unité des Agents Antibactériens, Institut Pasteur, Paris 75724, France.*
e-mails: djalal.meziane-cherif@pasteur.fr; patrice.courvalin@pasteur.fr

1. Kalan, L. & Wright, G. D. *Expert Rev. Mol. Med.* **13,** e5 (2011).
2. King, A. M. *et al. Nature* **510,** 503–506 (2014).
3. Woodford, N., Wareham, D. W., Guerra, B. & Teale, C. *J. Antimicrob. Chemother.* **69,** 287–291 (2014).
4. Drawz, S. M. & Bonomo, R. A. *Clin. Microbiol. Rev.* **23,** 160–201 (2010).
5. Fast, W. & Sutton, L. D. *Biochim. Biophys. Acta* **1834,** 1648–1659 (2013).
6. Lewis, K. *Nature Rev. Drug Discov.* **12,** 371–387 (2013).
7. Siemann, S. *et al. Biochim. Biophys. Acta* **1571,** 190–200 (2002).
8. Matsuura, A. *et al. Jpn. J. Pharmacol.* **63,** 187–193 (1993).
9. Courvalin, P., Leclercq, R. & Rice, L. B. (eds) *Antibiogram* (ASM Press, 2010).

FUNDAMENTAL CONSTANTS

A cool way to measure big *G*

Published results of the gravitational constant, a measure of the strength of gravity, have failed to converge. An approach that uses cold atoms provides a new data point in the quest to determine this fundamental constant. SEE LETTER P.518

STEPHAN SCHLAMMINGER

In our daily lives, we can see the effect of the gravitational force between Earth and an object, say an apple. However, the gravitational attraction between two apples cannot be observed without using a sensitive apparatus such as a torsion balance — it is just too small. On page 518 of this issue, Rosi *et al.*[1] describe an amazing measurement: the gravitational force between a rubidium atom and a 516-kilogram mass, with a relative uncertainty of just 0.015%. Their experiment was aimed at a precise determination of the gravitational constant, which describes the strength of the gravitational pull that bodies exert on each other, and was based on the technique of atom interferometry — a method that takes advantage of the wave nature of cold atoms to precisely measure gravitational acceleration.

In the atom interferometer described by Rosi and colleagues, a cloud of rubidium atoms at a temperature close to absolute zero is repeatedly tossed up vertically. To understand how this cloud in free fall probes gravity, quantum mechanics is needed. For simplicity, consider that the atoms in the cloud can be in two different atomic states, A and B. At the beginning, all atoms are in state A. By exposing an atom to an appropriately shaped light pulse, the atom can transition from A to B with a certain probability, let's say 50%. While the atom is not being observed, it is simultaneously in both states (50% in A and 50% in B), a concept known as superposition. In addition to inducing the transition from A to B, the light pulse transfers vertical momentum such that the B state has a larger vertical velocity than the A state.

The relative fraction of the two different states in this superposition varies with time, and its rate of change depends on the difference of the products of the momentum and the travelled vertical distance for each state. Owing to its larger momentum, state B travels higher than state A in the presence of the local gravitational acceleration, g, caused mostly by Earth and any masses in the vicinity of the cloud. Hence, the rate of change is a function of g. After the atomic cloud descends, close to the

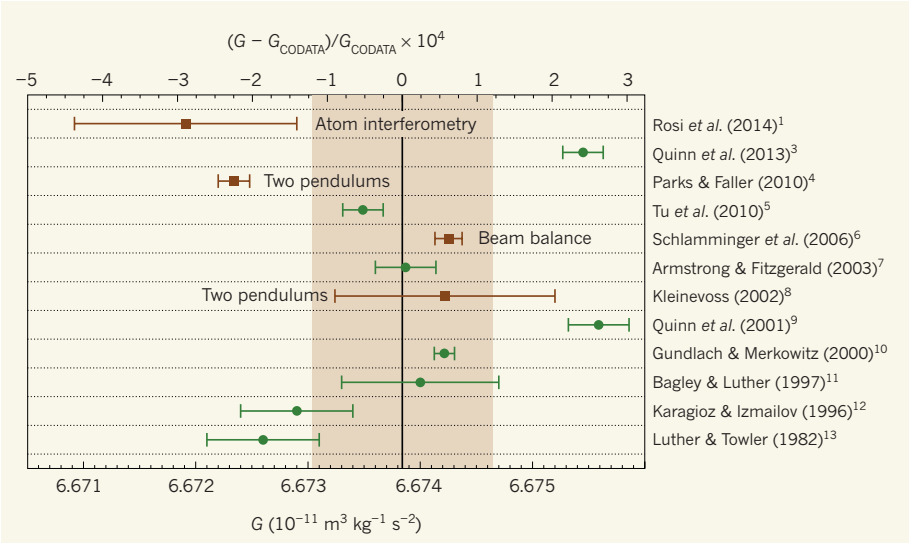

Figure 1 | The big picture for big *G*. Published results of measurements of the gravitational constant, *G*, over the past 32 years. The solid circles denote measurements that employed torsion balances. The three lower solid squares show results that were obtained using a beam balance or two pendulums. The upper solid square is the result obtained by Rosi and colleagues[1] using the technique of atom interferometry. The shaded area denotes the one-standard-deviation confidence interval of the value from the 2010 CODATA compilation of physical constants[18].

launch point, the ratio of the number of atoms in state A to state B is measured, from which g can be calculated[2].

To measure the gravitational constant G, an external mass, referred to as a field mass, is required. To understand the principle of the experiment we make two simplifications: we assume the field mass is a point with mass M, and that the atom interferometer measures g at one fixed point. In reality, the atom interferometer measured along a trajectory and cylindrical field masses were used. In this case, the idea is the same, although the maths is more complicated. The point mass is first located a distance z above the interferometer and the acceleration $g_{above} = -g + G(M/z^2)$ is measured. Next, the point mass is moved to a distance z below and $g_{below} = -g - G(M/z^2)$ is obtained. As long as g remains the same between the two measurements, G can be obtained from the difference between the measurements, $G = (g_{above} - g_{below})\, z^2/(2M)$. Unfortunately, g changes with time owing to tidal accelerations produced by the Sun and the Moon, air-pressure variations, and the movement of masses in the vicinity of the experiment.

To solve this problem, Rosi and co-workers measured g_{above} and g_{below} simultaneously by stacking two atom interferometers on top of each other. Two field masses were used and were at first in between the interferometers. The measured difference between g_{above} and g_{below} (the signal) is mostly independent of the temporal variation of g, but is dependent on its spatial variation, because the measurements were taken at different locations. The field masses were then moved such that one was above the upper interferometer and the other was below the lower interferometer, and the measurement was repeated. The difference between the signals in the latter field-mass configuration and the former one is independent of the spatial variation of g, and G was obtained by averaging about 100 such signal differences. The result is $G = (6.67191 \pm 0.00099) \times 10^{-11}$ cubic metres per kilogram per square second. The relative uncertainty of the measurement is 0.015%.

The experiment is exciting because it uses modern tools to solve an old problem. Using atoms to sense gravity instead of conventional mechanical devices, such as torsion balances, has several advantages. For example, the atom does not require a physical connection to the laboratory and is hence not biased by stray forces that such a connection would introduce to the measurement.

Naively, one would think that torsion balances are much better tools to precisely determine G than other devices. The torsion balances are much simpler in design and measure in a direction perpendicular to g, avoiding systematic effects caused by temporal variations of g. However, measurements performed over the past two centuries, mostly using torsion balances, have failed to converge on a trustworthy value of G. Figure 1 shows the results obtained in the past three decades. Out of the 11 results[3–13] shown, only three were measured with devices other than a torsion balance. One measurement was performed with a beam balance, a device that is typically used to measure mass, and two with pairs of pendulums. The relative difference between the largest and the smallest number is 0.055% — or about 40 times the size of the error bars of the experiment with the smallest uncertainty.

The various measurements of G seem not to converge on a value; it seems that the convergence gets worse with each additional data point. This is especially disconcerting because it is thought that G is a fundamental constant of nature. Although we cannot rule out for certain that the spread of the obtained values is caused by so far undiscovered properties of gravitation, this hypothesis seems unlikely because most plausible modifications to our theory of gravitation are excluded by other experimental tests. Adding more data points from isolated experiments has not been the best strategy to improve the situation. Instead, forming an international consortium[14] to coordinate these demanding experiments has been suggested.

Under the auspices of such a consortium, one or more apparatus can be sent to different institutions for measuring G. The different results and uncertainties could be compared. Such a procedure would provide insight into underestimation of uncertainties, the propensity to overlook bias in the experiment, and 'intellectual phase locking'[15], which is the tendency of an experimenter to stop looking for systematic effects once the measurement agrees with previously published results. By enhancing our understanding of these three human sources of error, which could be responsible for the spread shown in Figure 1, a more credible value of G can be obtained.

Rosi and colleagues' experiment provides an important data point in our quest to measure G (ref. 16). The experiment is vastly different from all other measurements, and the size of the achieved uncertainty, although still somewhat large, is approaching those obtained using torsion balances. Over the past 6 years, this team has reduced the uncertainty of their experiment by a factor of 10 compared with a preliminary result published in 2008 (ref. 17). Stay tuned, as they continue to push this technique to smaller uncertainties. ■

Stephan Schlamminger *is at the National Institute of Standards and Technology, Gaithersburg, Maryland 20899, USA.*
e-mail: stephan.schlamminger@nist.gov

1. Rosi, G., Sorrentino, F., Cacciapuoti, L., Prevedelli, M. & Tino, G. M. *Nature* **510,** 518–521 (2014).
2. Kasevich, M. & Chu, S. *Phys. Rev. Lett.* **67,** 181–184 (1991).
3. Quinn, T., Parks, H., Speake, C. & Davis, R. *Phys. Rev. Lett.* **111,** 101102 (2013).
4. Parks, H. V. & Faller, J. E. *Phys. Rev. Lett.* **105,** 110801 (2010).
5. Tu, L.-C. *et al. Phys. Rev. D* **82,** 022001 (2010).
6. Schlamminger, S. *et al. Phys. Rev. D* **74,** 082001 (2006).
7. Armstrong, T. R. & Fitzgerald, M. P. *Phys. Rev. Lett.* **91,** 201101 (2003).
8. Kleinevoss, U. PhD thesis, Univ. Wuppertal (2002).
9. Quinn, T. J., Speake, C. C., Richman, S. J., Davis, R. S. & Picard, A. *Phys. Rev. Lett.* **87,** 111101 (2001).
10. Gundlach, J. H. & Merkowitz, S. M. *Phys. Rev. Lett.* **85,** 2869–2872 (2000).
11. Bagley, C. H. & Luther, G. G. *Phys. Rev. Lett.* **78,** 3047–3050 (1997).

12.Karagioz, O. V. & Izmailov, V. P. *Izmer. Tekh.* **10,** 3–9 (1996).
13.Luther, G. G. & Towler, W. R. *Phys. Rev. Lett.* **48,** 121–123 (1982).
14.http://pml.nist.gov/bigg
15.Branscomb, L. M. *Am. Sci.* **73,** 421–423 (1985).
16.Quinn, T. *Nature* **505,** 455 (2014).
17.Lamporesi, G. *et al. Phys. Rev. Lett.* **100,** 050801 (2008).
18.Mohr, P. J., Taylor, B. N. & Newell, D. B. *Rev. Mod. Phys.* **84,** 1527–1605 (2012).

This article was published online on 18 June 2014.

STRUCTURAL BIOLOGY

Wobble puts RNA on target

Enzymes that attach amino acids to transfer RNAs during protein synthesis must recognize both substrates specifically. Crystal structures reveal a mechanism that explains the RNA specificity for one such system. SEE ARTICLE P.507

OSCAR VARGAS-RODRIGUEZ & KARIN MUSIER-FORSYTH

How genetic information encoded in nucleic acids is translated into amino-acid sequences in proteins has fascinated researchers for decades. Faithful translation involves specific pairing of triplets of nucleotides, called codons, in messenger RNA with complementary anticodons in transfer RNA. High accuracy also requires the attachment (aminoacylation) of each type of amino acid to a specific type of tRNA. Each variant of the aminoacylation reaction is catalysed by a particular aminoacyl-tRNA synthetase (ARS) enzyme, which must distinguish its own amino-acid substrate and the matching tRNA from the large pool of similar substrates. In this issue, Naganuma *et al.*[1] (page 507) report crystal structures that cast light on the remarkable mechanism by which information encoded in part of a tRNA is interpreted by an ARS, resulting in highly specific aminoacylation.

One of the simplest examples of tRNA recognition is that of alanyl-tRNA synthetase (AlaRS), the enzyme that attaches the amino acid alanine to its tRNA ($tRNA^{Ala}$). Across all domains of life, this recognition process relies primarily on a single 'wobble' base pair (designated G3·U70, where G and U represent the bases guanine and uracil, respectively) in a region of $tRNA^{Ala}$ called the acceptor stem[2,3]. The AlaRS·tRNA system has long been a model for studies of protein–RNA interactions and has been extensively investigated. Much was learned from these studies and from defining the three-dimensional structures of most of the other ARS·tRNA complexes, but a crystal structure of the AlaRS·$tRNA^{Ala}$ complex has been lacking. Naganuma and colleagues now report the crystal structure of AlaRS from the microorganism *Archaeoglobus fulgidus* in complex with $tRNA^{Ala}$/GU (the wild-type tRNA that contains the G3·U70 wobble pair), and that of a defective complex involving a mutant $tRNA^{Ala}$ that contains a standard Watson–Crick pair in place of the wobble pair ($tRNA^{Ala}$/AU).

Nucleotides that mark a tRNA for specific aminoacylation are known as tRNA identity elements, and the identity sets of tRNA-synthetase systems in bacteria are well understood[4,5]. In addition to the acceptor-stem domain, which is close to the site of amino-acid attachment, anticodons form part of the identity set for most tRNAs. The importance of the G3·U70 pair in AlaRS recognition, and the fact that the enzyme does not recognize the anticodon, helped to explain the early finding[6] that a $tRNA^{Ala}$ fragment derived from the acceptor stem is a substrate for aminoacylation by AlaRS, and led to speculation that a 'second genetic code' might determine the amino-acid specificity of tRNA molecules[7].

It was subsequently observed[8] that replacement of the wobble base pair with Watson–Crick base pairs greatly reduced the rate of catalysis (k_{cat}) of the aminoacylation of $tRNA^{Ala}$, rather than the binding affinity of AlaRS for $tRNA^{Ala}$. Specific chemical groups in and around the G3·U70 base pair[9,10] and distortion of the acceptor-stem helix of $tRNA^{Ala}$ (refs 11, 12) were also shown to have a role in recognition. These results left open the question of how discrimination by AlaRS was achieved largely through its effects on k_{cat}.

Naganuma and co-workers' structures reveal that AlaRS forms a homodimer (in which two identical subunits of the enzyme associate), and that each homodimer binds a single tRNA molecule. The tRNA interacts with three of the four domains of a single AlaRS subunit in an unprecedented orientation. The enzyme's carboxy-terminal domain binds $tRNA^{Ala}$/GU through interactions with the 'elbow' region of the L-shaped tRNA, and the aminoacylation domain interacts with the 3′-CCA end of the tRNA (a single-stranded region at the 3′ terminus that includes the point of attachment for alanine).

Duplex regions of RNA molecules, such as the acceptor stem of $tRNA^{Ala}$, contain two grooves known as the major and minor

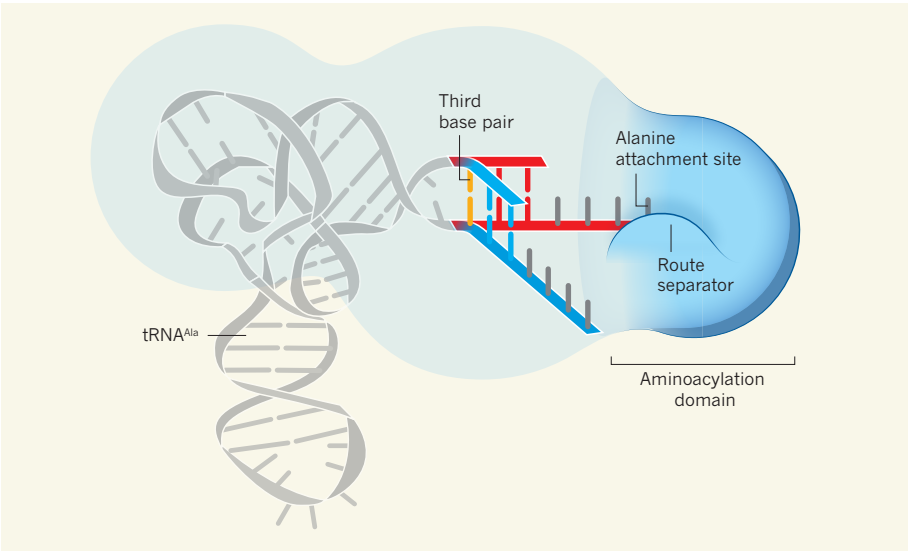

Figure 1 | Conformational effects of a single base pair in a transfer RNA. The AlaRS enzyme catalyses the attachment (aminoacylation) of the amino acid alanine to its matching tRNA ($tRNA^{Ala}$). Naganuma *et al.*[1] report crystal structures of AlaRS in complex with wild-type $tRNA^{Ala}$ (which contains a 'wobble' base pair in the third position of the acceptor-stem helix), and of AlaRS in complex with a mutant $tRNA^{Ala}$ that contains a Watson–Crick base pair instead of the wobble pair. In this cartoon, shaded regions indicate domains of AlaRS that contact the tRNA. The authors find that the acceptor-stem region of $tRNA^{Ala}$ adopts a straight conformation (red) when the wobble base pair is present, but a bent conformation (blue) with the Watson–Crick base pair. Only the straight conformation places the single-stranded region of the RNA into the active site of AlaRS's aminoacylation domain. Amino-acid residues in the aminoacylation domain act as a 'route separator' that prevents transition between the two conformations.